A&A manuscript no.
(will be inserted by hand later)

Your thesaurus codes are:
08.16.4, 08.13.2, 09.04.1, 09.16.1, 13.09.6

ASTRONOMY
AND
ASTROPHYSICS
24.9.1996

The rich spectrum of circumstellar PAHs*

D.A. Beintema[1], M.E. van den Ancker[2], F.J. Molster[2], L.B.F.M. Waters[2,1], A.G.G.M. Tielens[3], C. Waelkens[4], T. de Jong[2,1], Th. de Graauw[1], K. Justtanont[1], I. Yamamura[1], A. Heras[5], F. Lahuis[1,5], A. Salama[5]

[1] SRON Groningen, P.O. Box 800, NL-9700 AV Groningen, The Netherlands
[2] Astronomical Institute 'Anton Pannekoek', University of Amsterdam, Kruislaan 403, NL-1098 SJ Amsterdam, the Netherlands
[3] NASA Ames Research Center, Mail Stop 245-3, Moffett Field CA 94035, U.S.A.
[4] Instituut voor Sterrenkunde, Katholieke Universiteit Leuven, Celestijnenlaan 200B, B-3001 Heverlee, Belgium
[5] ESA Villafranca, P.O. Box 50727, E-28080 Madrid, Spain

received date; accepted date

Abstract. We present observations taken with the Short Wavelength Spectrometer (SWS) on board the Infrared Space Observatory (ISO) of three evolved C-rich stars, the post-AGB star HR 4049 and two planetary nebulae, IRAS21282+5050 and NGC 7027. The spectra are dominated by the well-known infrared emission bands, attributed to Polycyclic Aromatic Hydrocarbons (PAHs). The SWS spectra for the first time allow a complete overview of the richness of the PAH spectrum with high spectral resolution and high S/N. We present an inventory of the spectral features in the 2.4–17 μm wavelength window.

Key words: Stars: AGB and post-AGB – Stars: mass loss – Dust – Planetary Nebulae – Infrared: stars

1. Introduction

The presence of infrared emission bands at 3.3, 6.2, 7.7, 8.6 and 11.3 μm in the spectra of C-rich evolved objects has been known for over two decades (see e.g. *Interstellar Dust*, IAU symposium 135 (1989), eds. L.J. Allamandola & A.G.G.M. Tielens). These bands are due to C-C and C-H stretching and bending vibrations in an aromatic hydrocarbon material and various compounds have been proposed, which all have an aromatic microstructure in common (ie., PAHs, QCC, coal; Léger & Puget, 1984; Allamandola et al. 1985; Sakata et al. 1987; Papoular et al. 1989). Analysis of the energetics of the excitation/emission process has now firmly established that the carrier is quite small ($\simeq$ 50 C-atoms) and hence is properly referred to as PAH molecules (cf., Allamandola et al. 1989; hereafter referred to as ATB).

In this paper we present ISO-SWS observations of (proto) planetary nebulae ((P)PNe). We have selected three well-studied objects with a large range in excitation conditions, and for which high-quality ground-based spectra already exist, i.e. HR 4049 (e.g. Waters et al. 1989; Geballe et al. 1989; Roche et al. 1991; Buss et al. 1993) IRAS21282+5050 (e.g. de Muizon et al. 1986; Nagata et al. 1988; Witteborn et al. 1989; Jourdain de Muizon et al., 1990; Roche et al. 1991; Justtanont et al. 1996) and NGC 7027 (e.g. Gillett et al. 1973; Russell et al. 1977; Geballe et al. 1985; Nagata et al. 1988; Witteborn et al. 1989; Lowe et al. 1991; Sandford 1991). We present an inventory of the observed emission bands and a comparison with published data. We identify the emission bands in terms of the PAH hypothesis, but we stress that other components may also contribute to the bands. In an accompanying paper (Molster et al. 1996) we discuss shapes and strengths of some of the more prominent bands.

2. The observations

The observations were done with the Short Wavelength Spectrometer (SWS; de Graauw et al. 1996) on board ESA's Infrared Space Observatory (ISO; Kessler et al. 1996). Here we concentrate on the emission bands. Data reduction was carried out using version 4.1 of the SWS off-line processing pipeline. Flux calibration is believed to be accurate to about 10 percent at the shortest wavelengths, and 30–50 percent at 30–45 μm (Schaeidt et al. 1996). For a description of the wavelength calibration of SWS we refer to Valentijn et al. (1996). Figure 1 shows the spectra,

Send offprint requests to: D.A. Beintema

* Based on observations with ISO, an ESA project with instruments funded by ESA Member States (especially the PI countries: France, Germany, the Netherlands and the United Kingdom) and with the participation of ISAS and NASA

Table 1. Summary of observed bands

HR 4049				IRAS21282+5050				NGC 7027			
λmax (μm)	$F_\nu^\dagger$ (Jy)	fwhm (μm)	$F_b^\ddagger$	λmax (μm)	$F_\nu^\dagger$ (Jy)	fwhm (μm)	$F_b^\ddagger$	λmax (μm)	$F_\nu^\dagger$ (Jy)	fwhm (μm)	$F_b^\ddagger$
3.248	0.33	0.009	0.12	3.248	0.32	0.010	0.15				
3.296	5.13	0.045	9.24	3.294	2.13	0.040	2.82	3.287	19.8	0.037	20.2
3.342	0.22	0.021	0.21								
				3.397	0.54	0.030	0.78	3.398	3.49	0.024	2.70
3.423	1.17	0.036	1.77								
				3.435	0.41	0.012	0.24				
								3.467	0.70	0.014	0.45
				3.478	0.40	0.016	0.27	3.481	0.53	0.011	0.33
3.531	2.34	0.019	1.62	3.538	0.54	0.016	0.18	3.518	0.76	0.016	0.42
								3.546	0.62	0.008	0.15
				3.569	0.52	0.017	0.24	3.574	0.28	0.017	0.12
3.757	1.04	0.024	0.72								
				3.633	0.48	0.023	0.39	3.624	0.41	0.009	0.12
								5.234	8.00	0.114	11.3
								5.650	4.86	0.192	17.1
6.010	5.50	0.102	2.80	6.006	1.29	0.060	1.14				
6.258	14.5	0.165	26.2	6.217	11.4	0.168	17.9	6.219	51.6	0.150	68.4
6.318	2.06	0.024	0.36								
				6.940	2.33	0.257	4.62	6.924	1.37	0.217	16.4
7.602	4.89	0.076	1.14	7.609	2.22	0.106	1.29	7.594	15.7	0.150	9.63
7.892	23.56	0.496	47.1	7.724	12.3	0.486	32.4	7.815	75.1	0.554	174
8.068	2.00	0.059	0.87								
8.593	1.95	0.077	1.14								
8.679	12.5	0.250	12.8	8.626	7.96	0.351	7.98	8.585	42.7	0.320	31.8
9.707	5.06	0.112	3.78	9.533	2.49	0.721	7.47				
								10.44	5.81	0.398	55.5
11.04	7.85	0.102	3.36	11.05	4.08	0.096	1.38	11.05	18.0	0.080	5.64
11.26	15.9	0.152	9.75	11.23	24.6	0.243	15.1	11.22	238	0.215	125
				11.30	2.07	0.027	0.21				
11.67	2.73	0.068	0.60								
11.88	5.17	0.103	1.92					11.76	8.58	0.064	1.95
								11.95	13.0	0.102	5.04
				12.05	8.83	0.334	6.45				
12.75	5.19	0.487	6.90	12.63	13.2	0.469	23.6	12.73	71.6	0.449	79.8
				13.48	3.80	0.105	0.84	13.58	14.9	0.294	11.4
				16.99	13.3	1.087	20.1	17.03	36.0	0.694	43.2
				18.02	4.40	0.384	2.58	17.86	16.2	0.396	10.7

Notes to Table 1: † Peak flux; ‡ total flux in band, in 10^{-14} W m^{-2}.

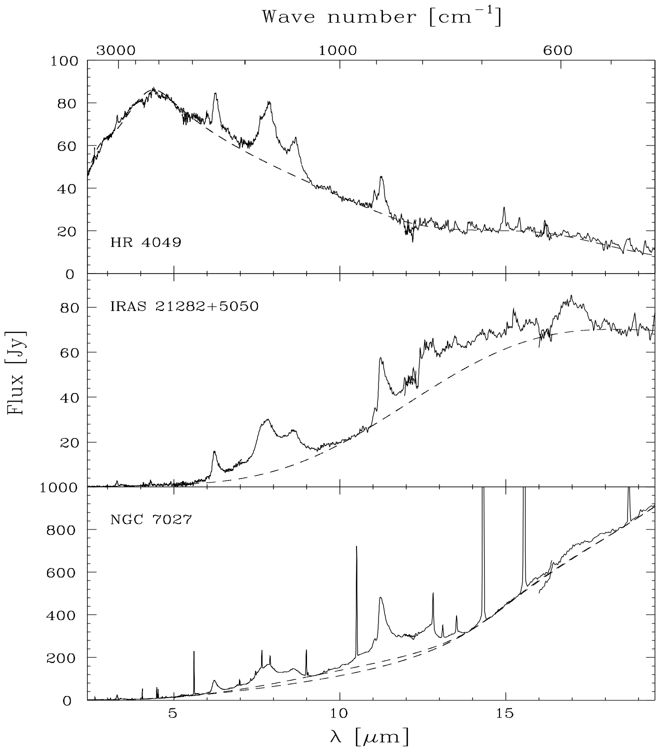

Fig. 1. SWS μm 2.4–20 μm spectra of the programme stars. The dashed lines indicate the location of the continuum.

rebinned to a resolution of 500, and Figure 2 the continuum subtracted spectra. We found that it is difficult to draw the continuum for NGC 7027 between 5 and 14 μm because the spectrum is dominated by emission bands. In Figure 1 two possible continua are drawn and Figure 2 shows the subtracted spectra for both cases. Note the richness in emission bands.

3. Comparison with ground-based data

Table 1 lists, for each star, the peak wavelength and FWHM (both in μm), the peak flux (in Jy) and the total flux in the band (in 10^{-14} W m^{-2}). The accuracy of the wavelength of the peak of the emission bands is about $\Delta\lambda/\lambda \approx 0.001$, and the band fluxes have an error of about 20 %. We stress that several bands severely blend (such as 7.7, 8.8, 11.05, 11.3 etc) and that this may affect the derived band strengths. We measured these band strengths with respect to the local continuum.

The spectrum of HR 4049 shows absorption bands at wavelengths of about 2.8, 4.2 and 4.6 μm. These bands could be due to gas-phase molecules, such as the ν_1 stretch vibrational band of H_2O (2.7–2.8 μm), CO_2 or SiO (near 4.2 μm), and the CO fundamental ro-vibrational band (near 4.6 μm). Evidence for CO absorption in the near-IR spectrum of HR 4049 was found by Lambert et al. (1988). We note that O-rich molecules are not expected in HR 4049 in view of the strength of the C-rich IR emission bands.

A comparison of groundbased (Geballe et al. 1989) and SWS spectra of HR 4049 in the 3 μm region shows that the 3.296, and 3.531 μm features in the SWS data agree well with the groundbased spectrum. The 3.405 μm feature seen by Geballe et al. does not appear to be present however. A prominent blue wing on the 3.296 μm peak is evident in the SWS data. Buss et al. (1993) discuss the 5–18 μm spectrum of HR 4049. The SWS spectrum agrees very well with their spectrum, both in flux level and strength of the features. The spectrum of Roche et al. (1991) shows that the 7.7–8.6 μm band has an extended wing to about 10 μm; this wing is resolved into a separate feature at 9.7 μm in the SWS spectrum. The shape of the 11.3 μm band of Roche et al. agrees well with our data; we confirm the presence of a 11.05 and a 12.7 μm feature.

The 3.3 μm spectrum of IRAS21282+5050 taken by Jourdain de Muizon et al. (1990) compares well with our SWS spectrum, despite the rather low S/N of the SWS spectrum in that wavelength region. The bands near 3.294, 3.397 and 3.569 μm are confirmed. The red wing

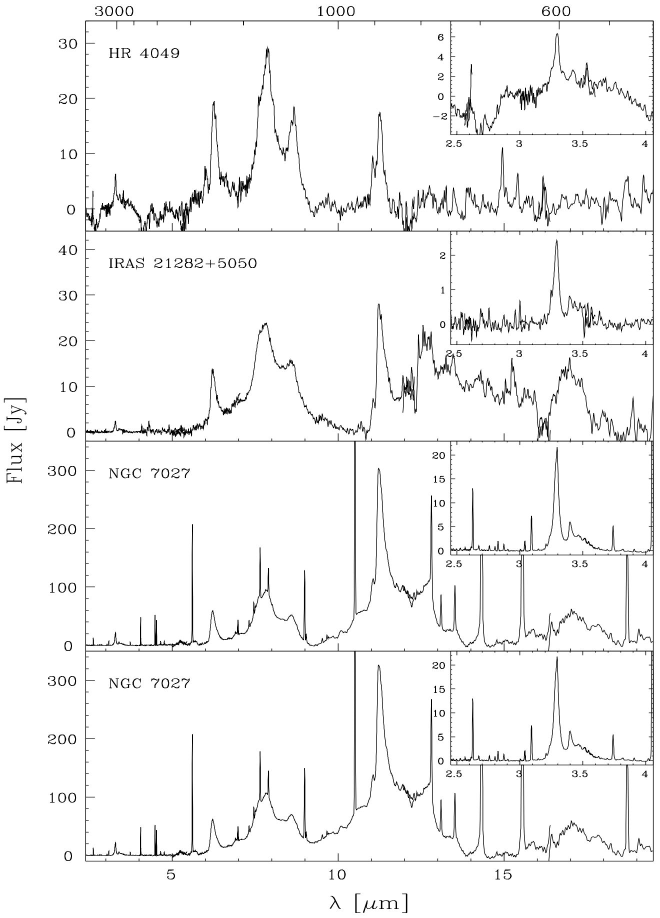

Fig. 2. Continuum subtracted spectra of the programme stars; the small panel gives the SWS 2.4–4 μm spectrum

on the 3.40 μm feature seen in ground-based spectra is resolved into a separate bump at 3.435 μm. The feature at 3.518 μm seen by Jourdain de Muizon et al. (1990) is not obvious in our spectrum, but this may be due to the presence of an AOT band edge near 3.50 μm (de Graauw et al. 1996). The feature at 3.478 μm is probably the same as that seen at 3.46 μm in ground-based spectra. Note the blue wing on the 3.294 μm C-H stretch. The 8–13 μm spectrum of IRAS21282+5050 taken by Roche et al. (1991) agrees with the SWS spectrum. The extended wing of the 7.7–8.6 μm bands is, as in the case of HR 4049, resolved into a separate feature near 9.5 μm. We confirm the presence of an extended wing out to about 13 μm, ending in the 12.7 μm band. We find a feature near 17 μm which is quite prominent, but was not found by Justtanont et al. (1996). The SWS relative spectral response curve has a complex shape around 17 μm which may cause spurious features.

Nagata et al. (1988) show a 3.3 μm spectrum of NGC 7027 with emission bands at 3.295, 3.396, 3.46 and 3.516 μm that we also see in the SWS data. However we do not find the 3.554 and 3.581 μm features seen by Nagata et al. (1988). The 10–13 μm spectrum of NGC 7027 published by Witteborn et al. (1989) shows the strong 11.3 μm feature which we resolve into two features at 11.05 and 11.21 μm. We find a feature at ~ 10.5 μm on which [S IV] λ 10.511 μm is superposed. The underlying plateau and the weaker bands near 11.0 and 12.7 μm were already noted in ground based spectra (Cohen et al. 1985; Witteborn et al. 1989; Roche et al. 1991). In addition, NGC 7027 shows a bump near 17 μm, similar to that seen in IRAS21282+5050, but which may be an artifact of the data reduction.

4. Identification of bands: the PAH hypothesis

The 3μm region: At the resolution and sensitivity of the SWS, the plateau in the 3μm region is resolved into several independent components and a number of new features are detected. This spectral region is dominated by the strong 3.294 μm feature due to the aromatic C-H stretch. Following the suggestion of Jourdain de Muizon et al. (1990), which was strengthened by arguments of Joblin et al. (1996), we attribute the 3.40 μm band to the asymmetric stretch in methyl groups attached to PAHs. The spectrum of methyl coronene also shows very weak bands near 3.35 and 3.48μm (Joblin 1992). There is no obvious sign of the three strong ethyl coronene bands in this wavelength region. Based upon the detection of the 2-0 overtone of the C-H stretch in IRAS21282+5050 (Geballe et al. 1994), the feature at 3.435 μm is assigned to the 2-1 hot band of the C-H stretch (Barker et al. 1987). In the same vein, the weak feature in IRAS21282+5050 at 3.59 μm may be due to the 3-2 C-H stretch. HR 4049 shows relatively strong features near 3.43 and 3.55 μm, which may well be the C-H hot bands. In that case, the 2-0 should be readily detectable in this source. Possibly, the smallest PAHs, which dominate the emission in these hot bands, survive better in the weaker UV radiation field of this source. The peak position of the aromatic C-H stretch is somewhat sensitive to molecular structure and internal excitation (cf., Joblin et al. 1995). The weak bands at 3.248 and 3.342 μm could thus be due to somewhat larger, less excited and somewhat smaller, more highly excited PAHs, respectively. There are a number of weaker features in these three spectra. These could be due to C-C overtone and combination bands (ATB). Other identifications are also possible. For example, the weak bands at 3.53 and 3.64 in NGC 7027 could be due to the C-H stretch in aldehydic groups attached to PAHs.

The 5–8 μm region: The strong “6.2” and “7.7” μm bands dominate this part of the spectrum and are assigned to aromatic C-C stretching modes (ATB). HR 4049 and to a lesser extent IRAS21282+5050 show a weak band at 6.0 μm. Perhaps, it is connected to the 3.248 μm feature. In any case, we would assign it to a (weak) C-C mode, possibly in a minor population of PAHs. The strong C=O stretching mode of aldehydic groups also absorbs in the 5.75–6.0μm region but generally peaks at somewhat shorter wavelength ($\simeq$ 5.8μm; Schutte et al. 1990). The "7.7" μm band shows evidence for two independent components at 7.6 and 7.8 μm (cf., Bregman 1989). The 6.9μm feature is quite evident in NGC 7027 (cf., Cohen et al. 1985). Non-compact PAHs show prominent C-C modes at this wavelength as do small compact PAHs (ie., pyrene). However, this band can also be due to deformation modes of peripheral CH_3 groups. We also recognize that these narrower features are perched upon a broad plateau which extends from about 5.5 to 10 μm, which is known to vary independently (e.g. Bregman et al. 1989). Perhaps, this plateau is due to blended C-C modes in larger PAH clusters ($\simeq$ 300–400 C-atoms). Finally, weak features at 5.23 and 5.65 μm are present in the spectrum of NGC 7027. These have been assigned to combination bands of the out-of-plane C-H deformation modes (Allamandola et al. 1989).

The 8–11μm region: Bands in this region are due to C-H in-plane deformation modes. The well known 8.6μm band dominates this spectral region. However, all three sources show evidence for weaker features, whose peak position varies between 9.5 and 10.5 μm depending on the H substitution pattern (Bellamy 1970). The observed pattern is consistent with the presence of isolated H's, as inferred from the out-of-plane C-H deformation mode. However, at this point, confusion with stretching vibrations of peripheral C-C and C=O groups cannot be excluded.

The 11–15 μm region: This is the region of the C-H out-of-plane deformation modes, which in interstellar spectra is dominated by the 11.3 μm band (Cohen et al. 1985). The 11.0 μm band may well correlate with the 6.0 and 3.248 μm bands. Bands in this region are very sensitive to the H-substitution pattern. Bands between 11 and 11.6 μm are generally assigned to peripheral H's isolated on the aromatic ring. The 12.7 μm feature is consistent with three adjacent H's (ATB), while the weak 12.1 μm band in IRAS21282+5050 can be assigned to duo H's. These assignments are somewhat under debate since these peak positions seem to be sensitive to ionization (Langhoff 1996) and this effect has not been sorted out completely, yet. The underlying broad plateau in NGC 7027 may represent a blend of various weak out-of-plane deformation modes, possibly connected to the larger PAH clusters. Finally, we note that this emission plateau extends to about 16 μm in IRAS21282+5050 (Justtanont et al. 1996) and that may be difficult to explain with out-of-plane deformation modes.

The long wavelength modes: Presently our data possibly reveal only one band, near 17 μm. This spectral 'poorness' may partly reflect the difficulty to detect (weak) emission features against the "dust" continuum which rapidly increases in strength with wavelength. Also, PAH modes in this wavelength region are intrinsically weak (ATB). Long wavelength bands are due to skeletal vibration and hence, in general, very specific for a particular PAH structure. As a corollary, this implies that, unlike the mid-IR spectral regions, bands from a collection of PAHs do not line up well, further hampering their detection. The 17 μm feature, if real, may well be the in-plane ring deformation mode. The out-of-plane ring deformation mode occurs at lower frequencies. The 21 μm feature observed in some sources may well be related to such vibration, which one might call the drumhead mode, where adjacent rings bend out-of-plane.

Acknowledgements. The authors thank the SWS Instrument Dedicated Team for their help in obtaining the spectra and in the data reduction. LBFMW acknowledges financial support from the Royal Netherlands Academy of Arts and Sciences, and from an NWO 'Pionier' grant. FJM acknowledges support from NWO grant 781-71-052.

References

Allamandola, L.J., Tielens, A.G.G.M., Barker, J.R.: 1985, ApJ 290, L25

Allamandola, L.J., Tielens, A.G.G.M., Barker, J.R.: 1989, ApJS 71, 733 (ATB)

Allamandola, L.J., Tielens, A.G.G.M., editors of IAU Symposium 135, *Interstellar dust*, 1989

Allamandola, L.J., Bregman, J.D., Sandford, S.A., Tielens, A.G.G.M., Witteborn, F.C., Wooden, D.H., Frank, D.: 1989, ApJ 345, L59

Barker, J.R.,Allamandola, L.J., Tielens, A.G.G.M.: 1987, ApJ 315, L61

Bellamy, L.J.: 1970, *The Infrared Spectra of Complex Molecules* (New York: John Wiley & Sons)

Bregman, J.: 1989, in *Interstellar Dust*, IAU Symp. 135, Eds. L. Allamandola & A.G.G.M. Tielens, p. 109

Bregman, J.D., Allamandola, L.J., Witteborn, F.C., Tielens, A.G.G.M., Geballe, T.R.: 1989, ApJ 344, 791

Buss Jr, R.H., Tielens, A.G.G.M., Cohen, M., Werner, M.W., Bregman, J.D., Witteborn, F.C.: 1993, ApJ 415, 250

Cohen, M., Tielens, A.G.G.M., Allamandola, L.J.: 1985, ApJ 299, L93

Geballe, T.R., Lacy, L.H., Persson, S.E., McGregor, P.J., Soifer, B.T.: 1985, ApJ 292, 500

Geballe, T.R., Noll, K.S., Whittet, D.C.B., Waters, L.B.F.M.: 1989, ApJ 340, L29

Geballe, T.R., Joblin, C., d'Hendecourt, L., Jourdain de Muizon, M., Tielens, A.G.G.M., Léger, A.: 1994, ApJ 434, L15

Gillett, F.C., Forrest, W.J., Merrill, K.M.: 1973, ApJ 183, 87

de Graauw, M.A. et al.: 1996, A&A (this volume)

Jourdain de Muizon, M., d'Hendecourt, L., Geballe, T.R.: 1990, A&A 235, 367

Joblin, C., 1992, Ph. D. Thesis, Université Paris 7

Joblin, C., Boissel, P., Léger, A., d'Hendecourt, L., Defourneau, D.: 1995, A&A 299, 835

Joblin, C., Tielens, A.G.G.M., Allamandola, L.J., Geballe, T.R.: 1996, ApJ 458, 610

Jourdain de Muizon, M., d'Hendecourt, L.B., Geballe, T.R.: 1990, A&A 235, 367

Justtanont, K., Barlow, M.J., Skinner, C.J., Roche, P.F., Aitken, D.K., Smith, C.H: 1996, A&A 309, 612

Kessler, M.F. et al.: 1996, A&A (this volume)

Lambert, D.L., Hinkle, K.H., Luck, R.E.: 1988, ApJ 333, 917

Langhoff, S,R.: 1996, J. Phys. Chem. 100, 2819

Léger, A., Puget, J.L.: 1984, A&A 137, L5

Lowe, R.P., Moorhead, J.M., Wehlau, W.H., Maillard, J.-P.: 1991, ApJ 368, 195

Molster, F.J. et al.: 1996, A&A (this volume)

Muizon, M. de, Geballe, T.R., d'Hendecourt, L., Baas, F.: 1986, ApJ 306, L105

Nagata, T., Tokunaga, A.T., Sellgren, K., Smith, R.G., Onaka, T., Nakada, Y., Sakata, A.: 1988, ApJ 326, 157

Papoular, R., Conrad, J., Giuliano, M., Kister, J., Mille, G.: 1989, A&A 217, 204

Roche, P.F., Aitken, D.K., Smith, C.H.: 1991, MNRAS 252, 282

Russell, R.W., Soifer, B.T., Willner, S.P.: 1977, ApJ 217, L149

Sakata, A., Wada, S., Onaka, T., Tokunaga, A.T.: 1987, ApJ 320, L63

Sandford, S.A.: 1991, ApJ 376, 599

Schaeidt, S. et al.: 1996, A&A (this volume)

Schutte, W.A., Tielens, A.G.G.M., Allamandola, L.J., Wooden, D.H., Cohen, M: 1990, ApJ 360, 577

Valentijn, E.A., et al.: 1996, A&A (this volume)

Waters, L.B.F.M., Lamers, H.J.G.L.M., Snow, T.P., Mathlener, E., Trams, N.R., van Hoof, P.A.M., Waelkens, C., Seab, C.G., Stanga, R.: 1989, A&A 211, 208

Witteborn, F.C., Sandford, S.A., Bregman, J.D., Allamandola, L.J., Cohen, M., Wooden, D.H., Graps, A.L.: 1989, ApJ 341, 270

This article was processed by the author using Springer-Verlag LaTeX A&A style file *L-AA* version 3.